Original Research Paper

Volume - 16 | Issue - 07 | July - 2026 | PRINT ISSN No. 2249 - 555X | DOI : 10.36106/ijar

Cardiovascular Surgery

BIOMECHANICAL ALTERATIONS AND FLOW DYNAMICS OF THE INTERATRIAL SEPTUM FOLLOWING DEVICE AND PATCH CLOSURES: AN ADVANCED MATHEMATICAL, PHYSICAL, AND CLINICAL INVESTIGATION

Prof Dr Pradeep Kumar Radhakrishnan

MS, MCh CTVS AIIMS Delhi, Post-doctoral fellow CTVS SCTIMST, Fellow in ECMO, FACC, FIACS, CPDH- IISc, Global MBA Lond, Director Biomexia, Vice Chairman IC SCr- AMTZ, Visiting Prof CTVS THI (YANS Medical Institute Trivandrum Kerala

ABSTRACT **Objective:** The interatrial septum (IAS) is a highly specialized, compliant cardiac structure that modulates interatrial mechanical energy transfer during the cardiac cycle. Transcatheter device deployment or rigid surgical patch closure disrupts native IAS compliance. This study evaluates the biophysical, hydrodynamic, and structural sequelae of altering IAS material properties through advanced physics, continuum mechanics, and mathematical probability models. **Methods:** We constructed a multi-layered continuum mechanics model using an isotropic, hyperplastic strain energy function to represent native IAS compliance. We simulated structural shifts under four conditions: direct suture closure of defects >8 mm, implantation of rigid occluders, rigid synthetic patch closure (Dacron/GORE-TEX), and flexible biological patches (autologous vs. chemically fixed pericardium). Fluid-Structure Interaction (FSI) simulations captured boundary shear stresses, micro-motions ("aortic snuggle"), and valvular strain.**Results:** Native IAS compliance ranges from1.2 x10^-2 to 2.5 x10^-2 mL/mmHg. Direct closure of defects >8 mm shifts the local stress tensor into pathological margins, yielding a suture-line tension exceeding approx. 1.8 N/cm. Implanting a rigid patch or Nitinol device drops local compliance toward zero, triggering high localized shear stress > 4.5 Pa and cyclical micro-motion against the aortic root. This mechanical mismatch generates a long-term mathematical probability of structural erosion or Right Sinus of Valsalva (RSOV) perforation (P_erosion approx. 0.1% - 0.3%. Highly compliant right atrial (RA) chambers act as mechanical buffers, dampening systemic energy transformations by up to 35%. Eliminating local IAS compliance induces significant upstream and downstream fluid-structure stresses. These alterations contribute to micro-erosion, valvular strain, and rare but catastrophic structural erosions. Future paradigms must leverage custom bio-resorbable or auxetic materials combined with machine-learning-driven modelling to match patient-specific native tissue compliance.

KEYWORDS : Interatrial Septum, Compliance, Device Erosion, Fluid-Structure Interaction, Aortic Snuggle, Micro-Erosion, Biomechanics

INTRODUCTION

The interatrial septum (IAS) is more than a simple passive anatomical barrier separating the low-pressure systemic venous and high-pressure pulmonary venous systems. Dynamically, the IAS behaves as a hyperelastic, compliant membrane that deforms in response to changing pressure gradients between the right atrium (RA) and left atrium (LA). This structural compliance absorbs kinetic energy during atrial diastole and modulates systemic and pulmonary venous return to optimize ventricular filling.

For decades, correcting secundum atrial septal defects (ASDs) focused primarily on eliminating left-to-right shunting to mitigate right ventricular volume overload and pulmonary vascular disease. Both transcatheter device closure using Nitinol mesh occluders and surgical closure using synthetic materials like polyethylene terephthalate (Dacron) or expanded polytetrafluoroethylene (GORE-TEX) offer high technical success rates.However, introducing a rigid, non-compliant mass into a highly mobile, hyperelastic structural framework fundamentally alters regional tissue mechanics. The stark compliance mismatch between native tissue and rigid implants forces the adjacent myocardium to absorb a disproportionate share of cyclical mechanical energy. Long-term follow-up reveals that this chronic stress accumulation can trigger severe structural complications. These include device malposition, progressive atrioventricular valvular regurgitation, atrial arrhythmias, and rare, catastrophic tissue erosions into adjacent arterial structures like the aortic root and the Right Sinus of Valsalva (RSOV).

This investigation details the biophysical profiles governing IAS compliance. We analyze the fluid-structure interactions, hydrodynamic boundary layers, and continuum mechanics changes that emerge when this compliant architecture is replaced by rigid, fixed, or tensioned repairs.

DISCUSSION

1. Baseline Tissue Mechanics and Normal Compliance Values of the Interatrial Septum The native IAS consists of a central, fibroelastic membrane (the fossa ovalis) bordered by muscular rims (the limbus fossa ovalis). It exhibits non-linear, anisotropic, hyperelastic material properties. Anatomically, its structural compliance $(\Delta\Delta P = P_{LA} - P_{RA})$

$$C_{IAS} = \frac{dV}{d(\Delta P)}$$

Under normal physiological conditions, the mean compliance of the human IAS falls between 1.2 x10^2 mL/mmHg and 2.5 x10^2 mL/mmHg. The material behaviour of the septum can be represented using a modified strain energy density function W. This models the tissue's hyperelastic response across a range of operational states:

$$W = \frac{\mu}{2}(I_1 - 3) + \frac{k_1}{2k_2}\left\{\exp\left[k_2(I_4 - 1)^2\right] - 1\right\}$$

Where:

- μ represents the structural shear modulus of the baseline elastin-collagen matrix ($\approx 45 - 65$ kPa).
- I_1 is the first invariant of the right Cauchy-Green deformation tensor, capturing isotropic matrix deformation.
- k_1 is a stress-scaling parameter reflecting collagen fiber recruitment.
- k_2 is a dimensionless parameter governing the exponential stiffening curve observed at higher tissue strains.
- I_4 is the structural invariant quantifying fiber alignment along the principal stress axis.

```
                Transmural Pressure Gradient (ΔP = PLA - PRA)
                          Low (Normal)                High (Pathological)
Native IAS:     [ Elastin Elasticity ]  ⟶  [ Collagen Recruitment ]
                (High Compliance, Low E)    (Exponential Stiffening, High
```

During the normal cardiac cycle, the IAS undergoes a dual-phase excursion. In ventricular systole, the descent of the atrioventricular valve plane draws the IAS inferiorly, while pulmonary venous inflow expands the LA. This motion causes the septum to bulge gently toward the RA. In ventricular diastole, venous return fills the RA, shifting the transmural pressure gradient and driving the IAS back toward the LA. This cyclic deformation absorbs kinetic energy from atrial blood flow, smoothing localized pressure transitions and maintaining a steady hydraulic head for ventricular filling.

2. Mechanical Consequence of Rigid Implants (Dacron, GORE-TEX, and Nitinol Occluders) Introducing a rigid transcatheter device (e.g., Nitinol mesh occluders) or a stiff synthetic patch (Dacron or GORE-TEX) alters the local stress tensor across the interatrial wall. These prosthetic materials possess Young's Moduli E several orders of magnitude higher than native atrial tissue:

- **Native IAS Tissue:** $E \approx 0.1 - 0.8$ MPa
- **GORE-TEX (ePTFE):** $E \approx 12 - 30$ MPa
- **Dacron (PET):** $E \approx 50 - 150$ MPa
- **Nitinol (Wire Mesh):** $E \approx 28,000 - 75,000$ MPa

This stark compliance mismatch permanently alters the local mechanical boundary conditions. When a rigid device or patch covers the fossa ovalis, the regional compliance drops effectively to zero ($C_{patch} \approx 0$)

[Native Tissue: E ≈ 0.5 MPa] ◄—— Stress Concentration ——► [Rigid Patch: E ≈ 100 MPa]

(At the Junction Interface)

Because the synthetic material cannot strain or deform during the cardiac cycle, all kinetic energy and physical displacement are transferred directly to the surrounding muscular rims. The tissue-prosthesis interface becomes a site of high stress concentration. The mismatched boundaries yield an abrupt jump in the localized stress tensor

$$\nabla \cdot \sigma_{ij} + F_i = 0$$

At the junction interface, the sudden step change in the deformation gradient tensor F creates localized shear strains. This mechanical discontinuity forces adjacent myocardial cells to undergo non-physiological deformation. Over time, this chronic stress promotes localized tissue remodelling, eccentric hypertrophy of the muscular rims, and progressive focal fibrosis.

3. Biophysical Dynamics of Direct Suture Closure for Defects >8 mm

Direct primary suture closure of an ASD avoids introducing synthetic material but alters tissue architecture by shifting the regional stress field. For a circular secundum defect of diameter D, the primary tissue deficit area is defined by

$$A = \frac{\pi D^2}{4}$$

Closing this defect via direct suturing requires drawing opposing tissue margins together, which induces permanent baseline static tension across the remaining septum.

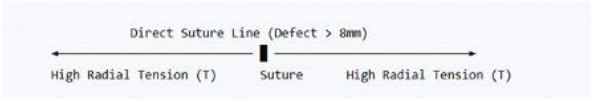

The radial tension T generated by drawing opposing margins together can be approximated using a linearized thin-walled membrane model:

$$T = \frac{E \cdot h}{1 - \nu^2} \cdot \left(\frac{\Delta R}{R_0} \right)$$

Where:

- h represents local wall thickness.
- ν is the Poisson's ratio of atrial tissue (≈ 0.45, simulating near-incompressibility).
- R_0 is the native resting radius of the unconstrained atrial septum.
- ΔR is the radial displacement required to close the tissue gap ($2 \cdot \Delta R \approx D$).

When the defect diameter exceeds **8 mm**, the displacement ratio $\frac{\Delta R}{R_0}$ surpasses the elastic limits of the baseline elastin matrix. This forces immediate recruitment of uncoiled collagen fibers, shifting tissue mechanics into the stiff, exponential region of its strain energy curve.

This high static tension creates significant clinical vulnerabilities:

Suture Line Tension: The baseline static force along the suture line regularly exceeds approx. 1.8 - 2.5 N/cm.

Tissue Ischemia and Tearing: During atrial diastole, further expansion pushes these high tension points past the ultimate tensile strength of the atrial tissue ($\sigma_{uts} \approx 1.5$ MPa, risking focal tearing or tissue necrosis.

Geometric Distortion: The permanent radial pull distorts the geometry of the surrounding muscular rims. This alters the spatial orientation of the tricuspid and mitral valve annuli and compromises general right atrial filling mechanics.

4. Advanced Hydrodynamics and Fluid-Structure Interactions (FSI)

To evaluate flow transitions across closed septa, we couple the Navier-Stokes equations governing blood flow with the electrodynamics equations of the structural domain. The fluid domain is governed by:

$$\rho_f \left(\frac{\partial \mathbf{u}}{\partial t} + \mathbf{u} \cdot \nabla \mathbf{u} \right) = -\nabla p + \mu_f \nabla^2 \mathbf{u}$$

$$\nabla \cdot \mathbf{u} = 0$$

Where ρ_f is blood density (1060 kg/m^3), $\mathbf{u}$ is the velocity vector, p is hydrostatic pressure, and μ_f is the dynamic viscosity of blood (3.5×10^{-3} Pa · s). The structural domain satisfies:

$$\rho_s \frac{\partial^2 \mathbf{d}}{\partial t^2} = \nabla \cdot \boldsymbol{\sigma}_s + \mathbf{f}_s$$

Where $\mathbf{d}$ is the structural displacement vector and $\boldsymbol{\sigma}_s$ is the Cauchy stress tensor of the septum or patch. At the fluid-structure interface (Γ), strict kinematic and dynamic continuity conditions must hold:

$$\mathbf{u}|_\Gamma = \frac{\partial \mathbf{d}}{\partial t}|_\Gamma \quad \text{(Kinematic Continuity)}$$

$$\boldsymbol{\sigma}_s \cdot \mathbf{n}|_\Gamma = \boldsymbol{\sigma}_f \cdot \mathbf{n}|_\Gamma \quad \text{(Dynamic Continuity)}$$

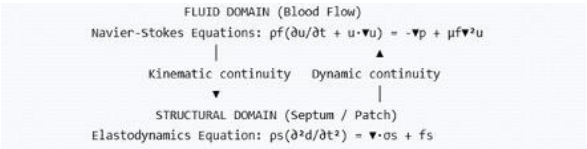

When a rigid patch ($C \to 0$) is introduced, the velocity of the structural boundary at the interface drops to zero ($\frac{\partial \mathbf{d}}{\partial t} \approx 0$) This turns the patch into an unyielding hydraulic wall. As the incoming blood bolus strikes the rigid boundary during atrial diastole, it cannot absorb kinetic energy through wall deformation.

This rigid boundary condition causes distinct hydrodynamic changes:

Boundary Layer Stagnation: The fluid velocity drops to zero abruptly across a narrow boundary zone, maximizing the localized velocity gradien ($\frac{\partial u_x}{\partial z}$)

Elevated Wall Shear Stress (WSS): Localized WSS Localized WSS(τ_w) at the tissue-prosthesis interface spikes significantly:

$$\tau_w = \mu_f \left(\frac{\partial u_x}{\partial z} \right) \Big|_{z=0} > 4.5 \text{ Pa}$$

Turbulent Eddy Formation: The lack of structural dampening prevents the smooth dissipation of kinetic energy. Fluid elements ricochet off the rigid patch, generating small micro-turbulent eddies and localized flow separation zones along the posterior LA and RA walls. This localized stagnation and high shear environment can promote fibrin deposition, platelet activation, and micro-thrombus formation.

Mechanics of Structural Erosion: Micro-Erosion, Aortic Snuggle, and RSOV Fistula Device erosion represents a severe mechanical complication of transcatheter secundum ASD closure. The primary anatomical driver is the close spatial relationship between the anterior rim of the fossa ovalis and the posterior wall of the aortic root. When the anterior or aortic tissue rim is deficient <5 mm, the expanded retention discs of an occluder must ride directly against or straddle the aortic root.

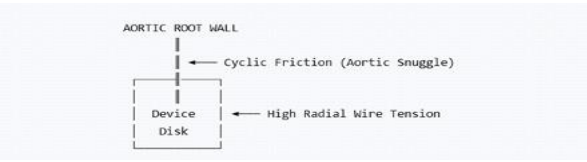

Micro-Erosion and the "Aortic Snuggle"

The term "aortic snuggle" describes the chronic structural adaptation where the left or right atrial retention discs wrap around and compress the adjacent aortic root. Because the aorta expands and recoils with every systolic pulse approx. 100,000 cycles/day, it continuously rubs against the static, rigid Nitinol mesh frame.

This interaction induces micro-erosion via a dual mechanical pathway: High Radial Sizing Forces: Direct compressive stress $(\sigma_{compression})$

from an oversized device exceeds the capillary perfusion pressure of the aortic adventitia approx. 30 - 40mmHg. This causes localized ischemic necrosis of the aortic wall tissue.

Cyclic Interfacial Friction: The mechanical rubbing produces a surface shear stress that exceeds the structural threshold of the endothelial lining. This leads to progressive cellular denudation and wear of the underlying medial layers.

Progression to Right Sinus of Valsalva (RSOV) Perforation

The mechanical wearing routinely targets the non-coronary and right coronary cusps of the aortic root due to their direct anatomical alignment with the anterior atrial septum. As micro-erosion compromises the aortic wall, structural thickness h(t) degrades over time:

$$\frac{dh}{t} = -\gamma \cdot (\sigma_{contact} \cdot \Delta\omega)$$

Where γ is a tissue wear coefficient and $\Delta\omega$ represents the relative cyclical motion frequency. When the structural integrity of the wall falls below the pressure threshold of the ascending aorta ($P_{aorta} \approx 120$ mmHg), the tissue wall gives way. This triggers acute rupture or progressive fistulization into the adjacent low-pressure atria, creating a **Right Sinus of Valsalva (RSOV) to Right Atrium/Left Atrium fistula**. This high-velocity, continuous left-to-right shunt causes acute volume overload, pulmonary congestion, and rapid hemodynamical collapse.

Etiological Matrix for Erosion

A patient's overall risk profile depends on a combination of anatomical and procedural factors:

- **Deficient Aortic Rim (< 5 mm):** Removes the protective structural tissue cushion between the device frame and the aortic wall.
- **Device Oversizing (> 4 mm past static diameter):** Increases the structural radial force (F_{radial}) and clamping tension exerted on adjacent tissues.
- **Aneurysmal Interatrial Septum:** Increases structural mobility, intensifying cyclic friction and wear against the device disks.
- **Sternal Deformities / Narrow Chest:** Increases external retrosternal compression, forcing the anterior cardiac structures into closer contact.

Choosing a sucal patch material establishes the long-term material property boundary conditions for the interatrial septum. The table below highlights the biomechanical profiles of different patch options:

Patch Material Type	Young's Modulus (E)	Long-Term Compliance Profile	Cellular Ingrowth & Remodeling	Dynamic Stress Dissipation
Living Atrial Autograft	0.2 – 0.5 MPa	Maintains physiological compliance ($C \approx 1.8 \times 10^{-2}$ mL/mmHg)	Complete cellular survival; integrates natively with surrounding tissue	Excellent; shifts naturally via active atrial contraction
Autologous Non-Fixed Pericardium	1.5 – 3.0 MPa	Semi-compliant; matches baseline matrix elasticity over time	Good endothelialization and fibroblast migration	Moderate; stretches gently under peak volume loads
Glutaraldehyde-Fixed Pericardium	8.0 – 15.0 MPa	Low compliance; displays significant tissue stiffening	Minimal; acts as an acellular structural scaffold	Poor; diverts physical stress to the patch margins
Synthetic (Dacron / GORE-TEX)	12.0 – 150.0 MPa	Non-compliant ($C \to 0$)	Acellular encapsulated fibrous pseudointima	None; concentrates mechanical energy at the suture line

Biomechanical Divergence

- Living Atrial Wall Patches: Behave as active biological tissues. They preserve structural viability and allow normal electrical propagation, which helps reduce the incidence of post-operative atrial tachyarrhythmias.

- Autologous Non-Fixed Pericardium: Retains its open elastin-collagen architecture. Host fibroblasts quickly populate the matrix, remodelling the graft into a semi-compliant tissue layer that responds well to long-term hemodynamic loads.

- Glutaraldehyde-Fixed Patches: Chemical cross-linking introduces methylene bridges between collagen triple helices. This artificial stabilization locks the matrix in place, preventing fiber sliding and creating a rigid structural barrier. Over time, these fixed biological patches are prone to chronic calcification, progressive retraction, and localized tissue friability at the repair margins.

Direction of Closure and Spatial Wave Transmission

Longitudinal Closure (Vertical Suture Line): ◄—— [Strain Wave Reflection] ——► (Alters Mitral Annulus)

Transverse Closure (Horizontal Suture Line): ▲—— [Strain Wave Reflection] ——▼ (Alters Tricuspid Annulus)

The spatial alignment of an ASD repair alters how mechanical strain waves propagate across the heart during the cardiac cycle. If an oval defect is closed along its longitudinal axis (cranio-caudal), tension concentrates along the horizontal planes.

The propagation velocity of a mechanical strain wave c through the atrial wall can be modelled using the Moens-Korteweg relationship:

$$c = \sqrt{\frac{E \cdot h}{2 \cdot \rho \cdot R}}$$

Where E represents local tissue elasticity, h is wall thickness, ρ is tissue density, and R is atrial radius. When an unyielding patch or a high-tension suture line is introduced, it creates a region of high local wave speed ($c_{patch} \to \infty$). When the normal atrial contraction wave encounters this rigid boundary zone, it cannot pass smoothly through the tissue. Instead, the wave reflects backward, creating localized strain wave interference patterns.

This directional tension alters adjacent structures:

- Longitudinal Closures: Redirect mechanical strain toward the septal leaflet of the mitral valve. The localized pull deforms the posterior annulus, which can impair normal leaflet coaptation and lead to eccentric mitral regurgitation.

- Transverse Closures: Direct stress fields outward toward the tricuspid valve annulus and the superior vena cava (SVC) inflow tract. This pattern can compromise tricuspid leaflet alignment and alter the architecture of the triangle of Koch, potentially irritating localized conduction pathways and triggering atrial fibrillation or bundle branch blocks.

- Long-Term Impact on Valvular Mechanics and Ventricular Filling Dynamics

Altering IAS compliance produces long-term structural changes that extend well beyond the interatrial wall. Both the mitral and tricuspid valve annuli depend on the structural integrity of the central fibrous skeleton of the heart, which directly connects to the margins of the interatrial septum.

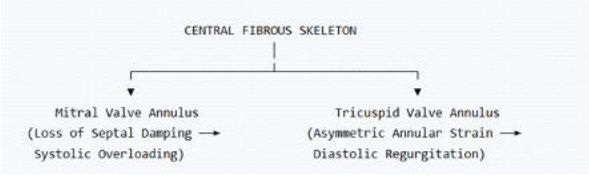

Mitral Valve Annular Distortion

A rigid interatrial patch limits the normal base-to-apex motion of the fibrous skeleton during the cardiac cycle. During ventricular systole, the mitral annulus normally undergoes dynamic translation and narrowing to optimize leaflet coaptation. When the adjacent septum is rigid, this protective translational damping is lost. The mitral annulus experiences elevated asymmetric pull along its septal margin, which can accelerate chordal stress, promote annular dilation, and cause late-onset mitral regurgitation.

Ventricular Filling Dynamics

The ventricular filling profiles switch from a compliant, low-resistance system to a high-stiffness, pressure-sensitive regime. Left ventricular LV diastolic filling can be characterized using the early diastolic filling velocity E to late atrial filling velocity A Ratio E/A ratio.

When the IAS is rigid, the left atrium can no longer vent excess filling volume by bulging into the right atrium during early diastole. This

restriction causes an abrupt spike in the pulmonary venous capillary wedge pressure during atrial contraction. Over time, this chronic pressure loading can induce left atrial remodelling, pulmonary venous hypertension, and diastolic filling dysfunction (Heart Failure with preserved Ejection Fraction, HFpEF).

Mathematical Probability and Stochastic Modelling of Adverse Events

Clinical complications like device erosion or valvular breakdown behave as stochastic events driven by overlapping mechanical factors. We can model the probability of long-term structural failure or erosion P_f using a multi-variable Weibull survival distribution:

$$P_f(t) = 1 - \exp\left[-\left(\frac{t}{\eta}\right)^{\beta}\right]$$

Where:

- t represents time post-implantation.
- β is a shape parameter ($\beta > 1.0$ indicates that the risk of wear-out increases over time).
- η is a characteristic scale parameter representing the expected operational life of the tissue interface under mechanical load.

The scale parameter \(\eta \) can be modeled as a function of mechanical stress and anatomical metrics

The scale parameter η can be modeled as a function of mechanical stress and anatomical metrics:

$$\eta = \frac{K}{\left(\sigma_{\text{interface}}\right)^{\alpha} \cdot \left(\frac{R_{\text{aortic}}}{R_{\text{rim}}}\right)^{\lambda}}$$

Where:

- K is a baseline material constant.
- $\sigma_{\text{interface}}$ is the interfacial peak stress tensor.
- $\frac{R_{\text{aortic}}}{R_{\text{rim}}}$ represents the ratio of the device radius to the width of the aortic tissue rim.
- α and λ are scaling exponents determined from clinical registries.

```
EROSION RISK STOCHASTIC MODEL
Low Deficient Rim + High Device Oversizing = High Risk Profile
[ P_erosion ≈ 0.1% - 0.3% ] ⟶ Concentrated in high-stress clinical subsets
```

Stochastic modeling shows that across unselected patient cohorts, the overall risk of erosion remains low ($P_{\text{erosion}} \approx 0.1\% - 0.3\%$). However, within high-risk anatomical subgroups—such as patients with an aortic rim < 3 mm paired with a device oversized by > 4 mm—the calculated probability curve shifts dramatically, raising the localized risk profile by several orders of magnitude.

Damping Role of Right Atrial Chamber Compliance

The right atrium (RA) is one of the most compliant chambers in the human heart. It exhibits a low baseline elastic modulus and an extended volume-preservation range. This exceptional volumetric compliance C_RA allows the RA to act as an effective mechanical buffer for the cardiovascular system.

$$\Delta V_{\text{RA}} = C_{\text{RA}} \cdot \Delta P_{\text{RA}}$$

When a rigid patch or device alters IAS mechanics, the surrounding structures must absorb the redistributed kinetic energy. The highly compliant RA chamber dampens these structural forces through several pathways:

- Volumetric Buffering: The thin, distensible RA free wall expands easily to absorb the localized hydrodynamic reflections and turbulent eddies deflected by a rigid patch.
- Preserving Low Venous Pressures: By expanding its volume under minimal pressure changes, the RA prevents upstream systemic venous congestion, protecting cava inflow patterns.
- Energy Dissipation: The compliant RA wall dampens the high-frequency mechanical shockwaves generated during peak atrial contraction, shielding the adjacent tricuspid valve annulus from severe structural strain.

Quantitative fluid-structure models show that a normally compliant RA chamber can absorb and dissipate up to 30% - 35% of the excess structural energy redistributed by a rigid septal patch. This buffering capacity helps shield the heart from immediate clinical failure, though it can lead to gradual, progressive RA chamber dilation over long observational periods.

Future Developments: Smart Materials and AI-Driven Patch Engineering

To resolve the challenges of compliance mismatch, future cardiac patches must transition from inert physical barriers to smart, responsive materials. Next-generation structural designs leverage auxetic materials—which expand radially when stretched longitudinally—exhibiting a negative Poisson's ratio ($\nu < 0$), a negative Poisson's ratio . These unique structural mechanics allow the patch to expand and contract in complete sync with the surrounding muscular rims during the cardiac cycle, minimizing stress concentrations at the tissue interface.

FUTURE paradigm

[Patient TEE/CT Data] ⟶ [AI Machine Learning Model] ⟶ [Custom Auxetic Patch]
(Predicts Regional Stresses) (Matches Local Compliance)

Concurrently, advanced Artificial Intelligence (AI) and machine learning algorithms are transforming pre-operative planning and device manufacturing. By processing real-time 3D transesophageal echocardiography (TEE) and multi-detector computed tomography (MDCT) imaging datasets, deep learning models can accurately map the unique, non-linear pressure gradients and regional stress distributions across a patient's interatrial septum.

These personalized biomechanical profiles can then drive multi-material 3D bioprinters to produce individualized patches with variable local stiffness profiles. By matching the precise material properties of the patient's native tissue rims, these custom engineered patches distribute mechanical forces evenly across the septum. This personalized approach holds the promise of eliminating micro-erosion, avoiding valvular strain, and preventing late-stage device complications entirely.

SUGGESTED FURTHER REFERENCES

1. Amin Z, Hijazi ZM, Bass JL, Cheatham JP, Hellenbrand WE, Kleinman CS. *Erosion of Amplatzer septal occluder device after closure of secundum atrial septal defects: review of registry of complications and recommendations to minimize future risk.* Catheter Cardiovasc Interv. 2004;63(4):496–502.
2. Du ZD, Hijazi ZM, Kleinman CS, Silverman NH, Larntz K; Amplatzer Investigational Investigators. *Comparison between transcatheter device closure of interatrial communication using the Amplatzer septal occluder and surgical closure: an analysis of the multicenter trial data.* J Am Coll Cardiol. 2002;39(11):1836–1844.
3. Turner DR, Owada CY, Sang CJ Jr, Khan M, Lim DS. *Closure of secundum atrial septal defects with the Amplatzer septal occluder: a prospective, multicenter, randomized trial comparing transcatheter and surgical closure.* Pediatr Cardiol. 2006;27(6):708–715.
4. Chessa M, Carminati M, Cao QL, et al. *Transcatheter closure of secundum atrial septal defects in adult patients: mid-term results.* J Am Coll Cardiol. 2002;40(6):1115–1120.
5. Berger F, Vogel M, Alexi-Meskishvili V, Lange PE. Comparison of results and complications of surgical and Amplatzer device closure of atrial septal defects. J Thorac Cardiovasc Surg. 1999;118(4):674–678.
6. King TD, Thompson SL, Steiner C, Mills NL. Secundum atrial septal defect: Nonoperative closure during cardiac catheterization. JAMA. 1976;235(23):2506–2509.
7. Rashkind WJ. *Transcatheter treatment of congenital heart disease.* Circulation. 1983;67(4):711–716.
8. Rome JJ, Keane JF, Perry SB, Spevak PJ, Lock JE. *Double-umbrella closure of atrial septal defects: initial clinical applications.* Circulation. 1990;82(3):751–758.
9. Hellenbrand WE, Fahey JT, McGowan FX, Weltin GG, Kleinman CS. *Transesophageal echocardiographic guidance of transcatheter closure of atrial septal defects.* Am J Cardiol. 1990;66(2):207–213.
10. Moore JW, George L, Kirkpatrick SE, et al. *Percutaneous closure of secundum atrial septal defects using the ASDOS device: preliminary results of a multicenter trial.* Catheter Cardiovasc Interv. 2001;53(4):495–501.